Journal of Clinical & Experimental Cardiology

Steinmetz et al., J Clin Exp Cardiolog 2012, S:8
DOI: 10.4172/2155-9880.S8-008

Review Article Open Access

Non-Invasive Imaging for Congenital Heart Disease – Recent Progress in Cardiac MRI

Michael Steinmetz[1]*, Hendrik C Preuss[1] and Joachim Lotz[2]

[1]*Department of Pediatric Cardiology and Intensive Care Medicine, University Hospital Goettingen, Germany*
[2]*Department of Diagnostic Radiology, University Hospital Goettingen, Germany*

Abstract

Cardiac magnetic resonance imaging (CMR) has become an important tool in evaluating congenital heart disease (CHD) in children and adults. By learning more about the advantages and limitations of CMR, clinicians and surgeons increasingly use the images and data acquired by CMR for the management of patients with CHD. MRI technology is evolving fast, and techniques such as 3D-MR angiography, phase contrast flow measurements, functional images to quantify cardiac function and stress testing are nowadays integrated parts of clinical care for patients with CHD. New technologies involve 4D-Flow measurement, "real-time" MRI or as a more future perspective MRI based catheter interventions.

This article intends to give an overview over the role of CMR in CHD, with a special focus on the latest development of the past 5 years and an outlook to the techniques on the horizon.

Abbreviations: 3D/ 4D: Three/ Four Dimensional; AAO: Ascending Aorta; APA: Atrio Pulmonary Anastomosis; APVR: Anomalous Pulmonary Venous Return; ARVC: Arrhythmogenic Right Ventricular Cardiomyopathy; ASO: Arterial Switch Operation/ Jatene Procedure; AV: Atrio-Ventricular; ccTGA: Congenitally Corrected TGA; CHD: Congenital Heart Disease; CMR: Cardiac Magnetic Resonance Imaging; CoA: Coarctation of the Aorta; CT: Computed Tomography; DAO: Descending Aorta; ECG: Electro Cardiogramm; EDV: End-Diastolic Volume; EF: Ejection Fraction; ESV: End-Systolic Volume; ET: Extracardiac Tunnel; GRE: Gradient-Echo; HO: Homograft; HOCM: Hypertrophic Obstructive Cardiomyopathy; ICD: Implanted Cardioverter Defibrillator; IVC: Inferior Caval Vein; LA: Left Atrium; LGE: Late Gadolinium Enhancement; LIT: Lateral Intracradiac Tunnel; LV: Left Ventricle; MAPSE: Mitral Annular Plane Systolic Excursion; MRI: Magnetic Resonance Imaging; NCC: Non-Compaction Cardiomyopathy; PA: Pulmonary Artery; PDA: Patent Ductus Arteriosus; PR: Pulmonary Regurgitation; PV: Pulmonary Valve; PVC: Premature Ventricular Contraction; Qp: Pulmonary Blood Flow; Qs: Systemic Blood Flow; RA: Right Atrium; RV: Right Ventricle; RVOT: Right Ventricular Outflow Tract; SSFP: Steady-State Free Precession; SVC: Superior Caval Vein; TAPSE: Tricuspid Annular Plane Systolic Excursion; TCPC: Total Cavo Pulmonary Connection; TGA: Transposition of the Great Arteries; TOF: Tetralogy of Fallot; VR: Virtual Reality; VSD: Ventricular Septal Defect

Introduction

Patients with congenital heart disease (CHD) are a challenge for imagers, since CHD requires a profound knowledge of the morphologic and functional characteristics of a broad range of congenital heart defects. Moreover, complex congenital heart disease often involves complex palliative or corrective surgery that alters the "normal" heart anatomy and cardiac function profoundly [1,2]. The number of patients reaching adulthood after correction or palliation of complex congenital heart disease is increasing significantly, thereby creating a whole new group of patients with complex chronic cardiac disorders [3,4].

Traditionally, imaging of CHD has been a domain of cardiac catheterizations and echocardiography. The last ten years have seen the rise of MRI and CT as accepted imaging modalities for congenital heart disease. Especially MRI has been the source of important insights into individualized pathophysiologic changes in CHD for both morphologic and functional aspects [5,6]. However, no single imaging modality has been shown to be able to obtain all information necessary for the complete evaluation of patients with CHD. Echocardiography is non invasive, possesses a high spatial and temporal resolution, but is often limited in its usability due to poor acoustic windows [3]. Assessment of valvular morphology and function is unmatched by any imaging modality in its temporal and spatial resolution [7].

In the cath lab, contrast agent volume and catheter position influence the degree of regurgitation, shunt magnitude, thereby introducing a bias and decreased stability in the assessment of cardiac functional parameters. However, invasive catheterization still remains the only reliable way for pressure mapping of the cardiac chambers and connected blood vessels as well as the assessment of coronary arteries.

Both modalities - echocardiography as well as invasive catheterization – have limitations in the assessment of complex anatomic alterations of the cardiac chambers and connected vessels. One of the main reasons for the success of MRI in the diagnosis and follow up of CHD is its ability to deliver detailed 3D imaging of the complex anatomy before as well as after surgical interventions [8].

Especially CMR has demonstrated added value of diagnostic accuracy in the functional assessment of the right ventricle as well as in its ability of imaging function and morphology in any spatial plane [9]. Minimal doses of contrast agents if any are needed for 3D angiography in CMR. In the recent years some concerns have been issued about the safety of MR contrast agents due to reports about nephrogenic

***Corresponding author:** Michael Steinmetz, MD, Department of Pediatric Cardiology and Intensive Care Medicine, University Hospital Goettingen, Robert-Koch-Str. 40, 37099 Gottingen, Germany, Tel: ++49-551-3922550; Fax: ++49-551-3922560; E-mail: michael.steinmetz@med.uni-goettingen.de

Received January 26, 2012; **Accepted** March 04, 2012; **Published** June 15, 2012

Citation: Steinmetz M, Preuss HC, Lotz J (2012) Non-Invasive Imaging for Congenital Heart Disease – Recent Progress in Cardiac MRI. J Clin Exp Cardiolog S8:008. doi:10.4172/2155-9880.S8-008

fibrosis caused by gadolinium based contrast agents. However, cyclic gadolinium based MR contrast agents are now considered safe and non-nephrotoxic in the young and grown-up patients. The lack of radiation exposure is an important advantage of MRI in comparison to multislice-CT or fluoroscopy.

Spatial resolution of CMR is inferior to multislice-CT or echocardiography. Most of the CMR-techniques employed today need multiple heart cycles to obtain all data needed. As a result functional data displayed are interpolations of multiple heart beats and not real-time acquisitions as compared to echocardiography. Therefore CMR imaging in the newborn and young children usually need intubation narcosis for high-resolution imaging. There are quite a number of sites that prefer deep sedation of the children up to the age of six limiting CMR exams to morphologic questions and accepting rough estimates for cardiac function. New developments allow for the synchronization of MR imaging with both breathing and cardiac motion.

MRI is quite sensitive to local disturbances of the magnetic field. Especially stainless steel and materials alike do induce severe disturbances of the local magnetic field yielding artifacts in the images that usually are much larger than the object causing them. These susceptibility artifacts are minimal with non-ferromagnetic materials like Nitinol. Stainless steel clips, valves, valve prostheses, stentgrafts all can cause susceptibility artifacts that can render an MRI exam nondiagnostic.

Techniques/ Imaging Sequences Available in CMR for Evaluation of CHD

Spin echo imaging with dark blood preparation

Anatomic imaging with high spatial resolution and suppressed blood signal. It helps to show anatomical relations of cardiac and extracardiac structures. In its fast variant, this sequence type can be used to image the whole chest in one to two breath holds with some compromises in image quality. Same sequence class can be used to look for myocardial edema.

Cine imaging

By ECG-triggered gradient-echo (GRE) and steady-state free precession (SSFP) sequences, a cardiac cycle can be resolved into multiple phases. These cine loops are recorded in defined planes and allow for quantification of cardiac function, mass and ventricular volumes. Moreover, qualitative assessment of wall motion, valve function, and identification of intra-cardiac or inter-vascular shunts is possible. Cine GRE measurements are more robust in terms of image quality and are better suited for the visualization of flow jets resulting from stenosis or insufficiencies. SSFP sequences provide a superb and homogenous contrast between blood pool and myocardium. SSFP sequences therefore are generally preferred for the visual and quantitative analysis of wall motion and cardiac function in general.

Velocity encoded phase contrast MRI for flow quantification

In- or through-plane measurements of flow velocity and thus quantification of cardiac output, stroke volume and calculation of shunt volume is possible [6,10]. To localize a high velocity intracardiac shunts or in the search of the maximum velocity, in-plane flow maps can be helpful.

3D- angiography with gadolinium enhancement

This technique is an excellent tool to show arterial and venous structures, shunt connections or anomalous vascular morphology or connections like aortic ectasia, coarction of the aorta, anomalous pulmonary venous drainage, focal or diffuse pulmonary artery stenosis, collaterals. It is also very helpful for 3D-visualization of the vascular anatomy to surgeons in preparation of complex surgical procedures and to exemplify the relationship to other cardiac and extracardiac structures [11].

Perfusion and dobutamine/ adenosine stress testing

Evaluation of myocardial ischemia due to coronary stenosis can be detected indirectly by perfusion imaging or wall motion analysis under pharmacologic stimulation. Perfusion imaging uses adenosine (140 µg/kg Bodyweight x min) to induce maximal dilation of the coronary arteries. During the dilation a short bolus of contrast agent is injected intravenously and the passage of the contrast agents through the myocardium is documented in a near-real time imaging. Coronary artery stenosis cause the dependent myocardium to remain darker than myocardium dependent on healthy coronaries as less contrast media finds its way beyond the stenosis.

Dobutamine stimulation is used in combination with wall motion analysis. Dobutamine is infused at increasing rate (5 to 40 µg / kg Bodyweight, steps of 10 µg every 5min). During every dobutamine level, wall motion is documented in MRI in at least 4 planes. Any new wall motion analysis under infusion of dobutamine is regarded as an evidence of a stenosis of the coronary artery supplying this myocardial wall segment.

Late gadolinium enhancement (LGE)

Late Gadolinuim Enhancement (LGE) is an integral part of imaging of cardiovascular disease and is found in a variety of cardiac diseases [12]. It helps to detect diseased myocardium from scars, fibrosis, deposition of material in extracellular space like amyloid, glycosides or alike. In congenital heart disease, LGE has been successfully used as a predictive indicator for ventricular function in patients after repair of TOF [13], TGA after arterial switch [14] or after Fontan palliation [15]. It has been found to be associated with increased risk of arrhythmias and sudden cardiac death in patients with hypertrophic cardiomyopathy [16] or coronary artery disease due to atherosclerosis [17] or surgical reimplantation [18]. Technically, late enhancement is based on a T1 weighted MR sequence with a special pulse to render normal myocardium black. The imaging sequence is done 12 to 15 min. after the injection of Gadolinium based contrast agent. Normal myocardium remains dark whereas diseased myocardium takes up various amounts of signal due to retained contrast material.

Early gadolinium enhancement

In comparison to Late Enhancement, the idea of Early Enhancement indicates a myocardial hyperemia or hyperperfusion as can be found in active myocarditis of any cause. Early Gadolinium Enhancement therefore is done immediately after the injection of intravenous contrast. As it might be difficult to visualize the subtle enhancement of hyperperfused myocardium, signal intensities of the myocardium are often compared to that of the pectoral muscles or paravertebral muscles.

Future Outlook/ Techniques on the Verge of Clinical Application

3D-/ 4D-Flow

Newer methods allow flow measurements of 3D-volumes thereby providing spatial and temporal resolutions of complex flow situations [19,20]. Data can be processed after the scan and flow or velocities can be measured at different locations within the data set. Especially palliated single ventricle anatomies with Fontan circulation have been looked at by 4D-Flow quantification [20]. Here, vortex formation and flow in the Fontan circulation may help determine prognosis and timing for intervention, surgery or heart transplantation [21]. However, further studies are needed to evaluate the use of this technique in clinical routine. Temporal resolution is inferior to that of 2D flow measurements and though quite some advances have been made, time required for a 3D flow measurement remains at 5 to 10 minutes.

Real time MRI

One of the major drawbacks of MR imaging is the lack of high-resolution real time image. It would allow MRI examinations not affected by arrhythmias and also enabling free breathing whilst obtaining high-resolution MR images of function or morphology. Several approaches have been proposed to the goal of real-time imaging. Echoplanar imaging has been employed but the images are susceptible to devastating artefacts and have inferior spatial resolution. Other approaches use highly accelerated imaging techniques like massive parallel imaging techniques in combination with sampling only a minute amount of data normally necessary for traditional MR imaging. Though insular solutions have been reported, real-time imaging still is in the laboratory phase and only available at specific research sites. It has been reported to help in the differentiation of constrictive versus restrictive myocardial disease by evaluation of the ventricular septal movement during valsalva manoeuvre.

MR based catheterization laboratory

Advances are being made in order to bring the advantages of invasive cathertization under fluoroscopy – interventions and invasive hemodynamics - to the CMR [22]. Various animal studies have demonstrated the feasibility of MR based catheterization techniques such as coronary intubation [23], balloon valvuloplasty of the aortic valve [24], fusion of x-ray and CMR-roadmaps for device based VSD-closure [25], intravascular angioplasty and stent placement [26-29] or assessment of ventricular function [30]. New CMR methods analogous to selective catheter-angiography to visualize flow using virtual dye are being developed [31]. Patient safety is the major concern in the development of interventional instrumentation. The development of CMR suitable catheters, stents, balloons and MR sequences is under way, but still not available for routine use in humans [22,31-33]. However, some investigators see the practical implementation of the MRI based catheterization lab on the horizon [34,35]. One important step to implement MRI based angiographies similar to those known from the conventional catheter lab using fluoroscopy would be a robust spatial as well as temporal real time MRI technique.

Whole heart sequences, 3 D reconstruction and 3 D hardprints for operation planning/ 3D virtual surgery

Virtual reality 3D-reconstruction is a standard tool in CMR. Newer techniques apply this for more detailed planning of surgery using rasin-based hardprints of the 3D-models so that a surgeon can physically put his hands on a and look at the complex anatomy from all sides according to the individual needs [36]. To take this even further, 3D-sequences are used to create models for virtual surgery, so that the surgeon may simulate his operation in a computed model before performing the surgery on the actual patient [37,38]. Although these are interesting and helpful techniques for a more individualized treatment, further steps to implement them in routine clinical practice will have to be done.

Special Congenital Malformations

Tetralogy of fallot (TOF)

Tetralogy of Fallot (TOF) is the most common cyanotic cardiac defect accounting for approx. 10% of all CHD. TOF patients have been examined by CMR more than any other group of patients with CHD. RV function and size, regional dysfunction, scarring, degree of pulmonary regurgitation (PR) and pulmonary arterial anatomy can be assessed reliably (Figure 1). These data are used increasingly for risk stratification and timing of repetitive valve replacements, interventions for peripheral pulmonary stenosis or antiarrhythmic therapy with drugs or pacemakers/ ICDs. Moreover, CMR is very useful to plan operative or interventional steps in the follow-up after TOF repair. 3D MR-angiography complements echo and catheterization techniques. CMR provides exact three dimensional virtual models of the RV, RVOT and the pulmonary arteries. In addition CMR in TOF also yields a wealth of functional parameters that have become essential in clinical decision making.

Oosterhof et al. have reported that RV EDV more than 160 mL/m^2 or RV ESV more than 82 mL/m^2 in CMR prior to repair of significant pulmonary regurgitation is associated with decreased chances of normalization of RV volume [39]. RV-Dilation >150-160 ml/m^2 with decreased RV function is now regarded an important cut-off parameter for the timing of pulmonary valve (PV) replacement. Gender specific normal CMR values for ventricular volumes and myocardial mass for children and adolescents have been published recently [40] as well as for patients after repair of TOF [41]. Gender specific percentiles of CMR parameters in patients with repaired TOF computed for an age range from 8 to 40 years show changes over time in LV volumes especially in females and RV volumes in both male and females. Also bi-ventricular ejection fraction (EF) decreased in male patients, whereas in female patients only RV EF decreased. This should be considered when defining thresholds for intervention. Gender-specific percentiles for the individual patient may help in finding the optimal time point for PV replacement [41].

The confounding influence of residual right ventricular outflow tract (RVOT) obstruction combined with pulmonary regurgitation (PR) vs. isolated PR after TOF-repair has also been addressed lately. Residual RVOT obstruction was associated with smaller RV-volumes and higher RV-EF. Thus, TOF patients with residual RVOT obstruction may need, earlier PV replacement, i.e. even when RV-volume is lower than 160ml/m^2 in CMR, compared to those with no RVOT obstruction [42].

Another predictor for RV function and increased risk of sudden cardiac death due to ventricular arrhythmia is the extent of ventricular fibrosis. This can be assessed by late gadolinium enhancement in CMR [13,15,43]. The more fibrosis detected in CMR by LGE, the higher the risk for sudden cardiac death and deteriorating RV function.

Intra-(RV) and inter-ventricular, as well as atrio-ventricular dependence has been addressed in recent CMR studies in repaired

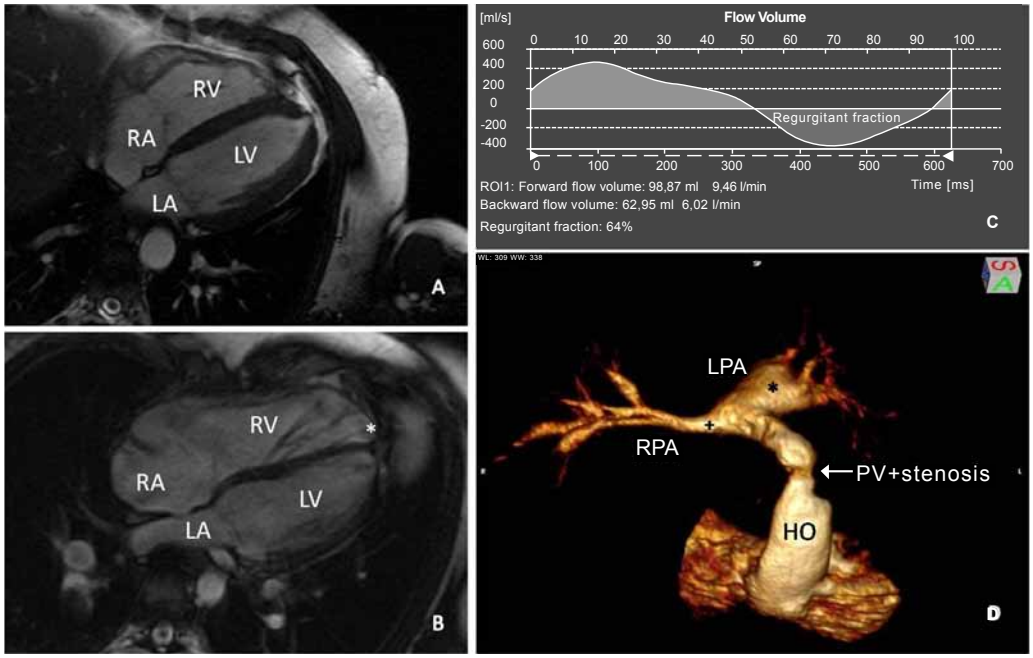

Figure 1: Tetralogy of Fallot.
A: 4 chamber view cine imaging with normal size of RV and LV. B: Enlarged RV and normal sized LV in a patient with pulmonary regurgitation after repair of TOF with transanular patch plasty. The apex is formed by the RV (*) while in a normally sized heart, it is formed by the LV. C: Volume change over time from flow measurement of the pulmonary trunk showing severe pulmonary regurgitation with 64% regurgitant fraction. D: VR 3D Reconstruction of the right ventricle and pulmonary arteries from MR angiography. Valvular and supravalvular stenosis in the homograft (HO) and stenosis of the RPA (+) with aneurysmatic enlargement of the LPA (*) in a patient with TOF after corrective surgery with pulmonary valve replacement by homograft.

TOF. Echocardiography parameters such as tricuspid- and mitral annular plane systolic excursion (TAPSE, MAPSE), speckle tracking and myocardial strain have been related to CMR findings. Their potential in routine clinical echo examination and their role as predictive parameters for the timing of necessary interventions has been evaluated [44-46]: A) The individual components of the RV react differently to volume overload [47]. B) Moderate systolic and diastolic right ventricular dysfunction appears to be associated with impaired right atrial function in TOF patients, which corresponds to decreased TAPSE in echocardiography [45]. C) Despite normal EF on CMR and echo, TOF patients exhibit a decreased 2D-longitudinal strain, suggesting subclinical functional impairment [44].

The accuracy of 3D-echocardiography has also been compared to CMR in TOF patients and has been shown to decrease significantly with increasing RV-sizes, while CMR values remain relatively robust [48].

CMR is also used to plan percutaneous pulmonary valve interventional (PPVI) replacement and document ventricular improvement in follow up examinations [49]. Of note, MRI based evaluation of pulmonary valve function can be limited after stent mounted interventional valve replacement, due to the artifacts produced by metal stents.

Coarctation of the aorta (CoA)

The congenital narrowing of the aorta is frequently located in close vicinity of the site of ductal insertion (aortic isthmus) [50]. In infancy and with critical coarctation the treatment of choice is surgery. Elder patients with less severe CoA and subjects with re-coarctation after initial surgical repair are eligible for interventional therapy using balloon angioplasty or stent implantation [51-53]. Follow up of patients after corrective surgery for CoA can be difficult if the patient reaches adult age. Echocardiography is very limited, once the patient is grown-up, and the aortic arch is only poorly visualized.

Recent studies show that a considerable number (up to 50 percent) of patients after corrective surgery for CoA develop aortic abnormalities. However, a significant number of these patients are asymptomatic [54]. A common complication after surgical repair of coarctation is the development of re-coarctation or aortic aneurysms. Patients with bicuspid aortic valves appear to be at a higher risk for developing re-coarctation whereas patients after surgical repair with patch plasty rather tend to develop aortic aneurysms [55-57]. It is therefore desirable to detect these abnormalities at an early stage in order to commence treatment before adverse effects can manifest or become irreversible.

CMR and MR angiography are excellent tools to evaluate left ventricular function, associated aortic valve malformation as well as aortic arch morphology. Residual coarctation or formation of aortic aneurysms can be detected reliably [58-60] (Figure 2). In addition, patients with CoA show a high prevalence of associated cardiovascular abnormalities which can also be detected using CMR imaging techniques like 3D SSFP sequences [58,61].

CMR imaging in patients with CoA also has high prognostic value regarding the likelihood of postoperative complications. Late systemic hypertension or re-coarctation after surgical repair appear to be predictable to some extent using aortic arch morphology and flow measurements [59,62-65]. New imaging techniques such as 4D flow measurements can be used to evaluate hemodynamic indicators like vortex formation, vascular strain and collateral-vessel-flow. These CMR techniques employed after surgical repair may help predict

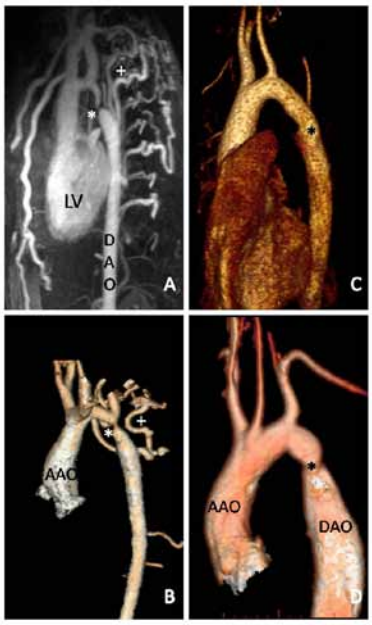

Figure 2: Aortic Coarctation.
A: MR angiography of native coarctation of the aorta in a 9 year old boy with subtotal stenosis at the level of the aortic isthmus (*) and multiple subclavian and intercostal collaterals (+) inserting into the descending aorta (DAO) distal to stenosis (AO= aorta). B: Virtual reality (VR) 3D reconstruction from MR angiograpy in a 6 year old girl with aortic coarctation (*) and collaterals (+). C: VR 3D reconstruction from MR angiography after surgical resection of aortic coarctation and end-to-end anastomosis. Only very slight residual narrowing at the site of the former stenosis (*). D: VR 3D reconstruction form MR angiography of re-stenosis (*) after surgical resection of aortic coarction and end-to-end-anastomosis. AAO = ascending aorta, DAO= descending aorta.

complications and determine the schedule for follow-up screenings or interventional therapy [66-68].

In patients with CoA after interventional therapy dedicated imaging sequences like gradient echo cine sequences using a high flip angle can be used to characterize coarctation stents and estimate stent-associated stenosis using 3D-angiography and phase-contrast flow mapping [69,70]. Still, depending on the material of the coarctation-stent used, there are limitations for the assessment of in-stent-stenosis and morphology using CMR, which may necessitate the alternative use of cardiovascular CT [71-73].

An interesting future prospect for the use of CMR in patients with CoA may be personalized 3D hemodanymic simulations based on CMR data. Possibly, this could help to determine whether a patient would benefit more from either surgery or interventional therapy. Using computer-generated hemodynamic simulations it would be possible to compare the changes in simulated hemodynamics after either procedure [68,74].

Transposition of the great arteries (TGA)

Transposition of the great arteries TGA is the second most common cyanotic heart defect after TOF. It is subdivided into simple and complex TGA. Depending on the position of the aorta, it is also subdivided into dextro (D) and levo (L or congenitally corrected (cc)) TGA.

Survival of patients with dTGA is dependent on sufficient mixing of oxygen saturated and depleted blood on the atrial level. This mixing is augmented by additional shunt connections that increase pulmonary vascular perfusion and thereby left atrial pressure (i.e. VSD, PDA). Surgically, patients with dTGA are nowadays corrected by the arterial switch operation (ASO). The procedure involves reposition of the great arteries to their corresponding ventricle (LeCompte maneuver), accompanied by excision and reimplantation of the coronary arteries, early in life.

The different forms of repair/ palliation present a challenge for the CMR examiner. For post operative follow up CMR can be most valuable.

TGA after anatomical correction by arterial switch operation (Jatene procedure): The arterial switch operation (ASO) can be associated with stenosis of the pulmonary artery due to the LeCompte maneuver, supravalvular stenosis of the aorta or pulmonary artery, aortic root dilatation, aortic valve regurgitation or coronary problems.

Vascular anatomy and valve patency are evaluated using cine imaging, MR-angiography with 3-D reconstruction and velocity encoded phase contrast techniques (Figure 3). Coronary morphology at least in the proximal part can be assessed by MR-angiography, too. The effect of coronary stenosis on myocardial perfusion can be seen in sequences involving perfusion stress imaging with adenosine or dobutamine.

Echocardiography and CMR have been compared in patients after arterial switch operation. Echocardiography underestimated RV function, image quality and visualization of the baffles was superior in CMR [75]. Unbalanced distribution of pulmonary blood flow due to pulmonary arterial branch stenosis after ASO appears to be associated with reduced exercise capacity and increased ventilator drive. CMR can help in differentiating the pulmonary artery lesions that are functionally important [76].

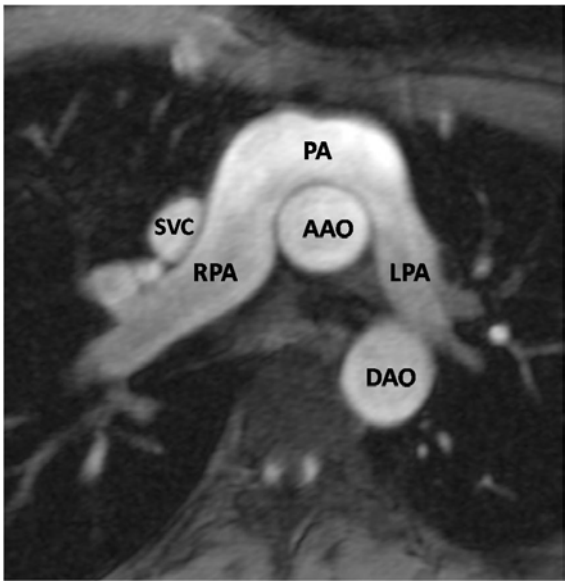

Figure 3: TGA.
TGA after arterial switch operation (ASO) and LeCompte maneuver . The pulmonary artery (PA) is brought anterior of the ascending aorta (AAO) and the LPA and RPA "flow" around the AAO. DAO=descending aorta, SVC=superior caval vein.

TGA after atrial switch procedure (Mustard or Senning procedure): Since the 1960's, patients have been or - if additional cardiac malformations exsist that make the arterial switch correction impossible - still are palliated by the atrial switch operation techniques such as Mustard or Senning procedures. These involve the creation of an intraatrial artificial tunnel that shunts desaturated blood from the caval veins to the left sided AV-valve and via the left ventricle to the pulmonary artery. Saturated blood from the pulmonary veins is shunted to the right sided AV-valve and via the right ventricle to the aorta.

The very unusual cardiac anatomy after atrial switch procedures can be assessed by cine and 3D-imaging in CMR. The venous baffle, RV- (systemic ventricle) and LV- (sub-pulmonary ventricle) function, baffle leaks or obstructions can be detected by CMR using cine imaging and inplane flow maps (Figure 4).

For patients late after Mustard/ Senning procedures, a correlation between CMR derived RV systolic and diastolic volumes, NT-proBNP and QRS duration on ECG has been shown [77]. Moreover, compared to congenitally corrected TGA (ccTGA), dTGA patients after atrial switch procedures cannot increase stroke volume during stress [78]. They also exhibit impaired ventricular filling as well as decreased contractility in dobutamine stress CMR [79]. The RV EF, QRS duration and incidence of arrhythmia have been shown to correlate with LGE detectable scar in patients after arterial switch operation and with congenitally corrected TGA (ccTGA) [14,80]. Function of the pressure unloaded LV (i.e. sub-pulmonary ventricle) after atrial switch has also been looked at by CMR: Decreased ventricular torsion and diastolic abnormalities have been implied to be measures of subclinical ventricular dysfunction [81]. Aortic function appears to be compromised in patients with TGA and atrial switch with significant dilatation of the aortic annulus and the sinus of Valsalva. The ascending aorta exhibits reduced distensibility in these patients. No correlation with RV size, function and mass in the young sample group could be demonstrated [82].

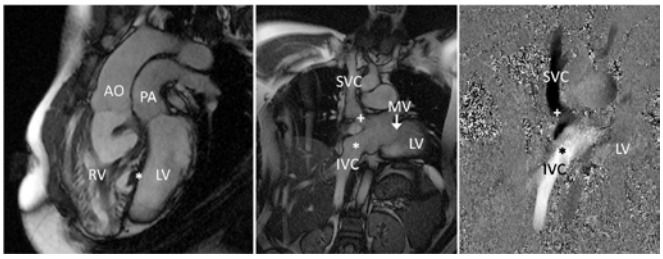

Figure 4: TGA.
TGA after atrial switch operation with Mustard procedure. A: The aorta (AO) is positioned anteriorly and arises from the hypertrophied, morphologically RV. The pulmonary artery (PA) is positioned posteriorly and arises from the LV, which is smaller and has less myocardial mass. The septum (*) is pertrudes into the LV due to increased RV pressure. B: Baffle view in TGA after Mustard procedure with a baffle from the SVC and IVC to the mitral valve (MV), with the superior (+) and inferior (*) baffle. C: In plane flow map of the same view.

Fontan circulation/ total cavo pulmonary connection (TCPC)

After univentricular palliation following the modified Fontan principle (TCPC), patients usually have to live with one ventricle that supplies the systemic circulation. The pulmonary circulation is maintained passively and aided by a suctioning component of the ventricle and by the varying intrathoracic pressure during in- and exspiration. CMR is very helpful in imaging the TCPC anatomy, identify stenosis at the anastomosis sites (usually right PA with SVC and IVC), assess ventricular function and valve patency and evaluate fibrosis as a predictive parameter (Figure 5A).

Reduced venous flow in CMR has been linked to suboptimal Fontan hemodynamics and failing Fontan circulation [83]. Venous flow and especially its pulsatility has been compared in atrio pulmonary anastomosis (APA), lateral intracardiac tunnel (LIT) and extracardiac tunnel (ET) Fontan modifications. As could be expected, APA was associated with more pulsatile flow, but also with increased backflow, atrial enlargement and occurrence of arrhythmia compared to LIT and ET [84]. Moreover, collateral flow has been identified as a contributor to enhanced pulmonary flow during stress, while decreased diastolic compliance is one cause of ventricular dysfunction [85]. Recently, 4D-Flow maps of Fontan circulation have been acquired (see picture 5 B-D) and different modifications such as the lateral tunnel and the extracardiac conduit have been compared with this technique. The different modifications exhibit different flow patterns and formation of vortices depending on the preceding operative steps (i.e. Glenn or Hemifontan) [86]. These studies may help to determine the effect of flow dynamics - seen also in conventional angiography and evaluated subjectively – on the long term function of Fontan circulation. However, further studies are necessary to implement these findings into clinical practice. Exercise capacity of Fontan patients is usually lower than that of healthy children or adults in the corresponding age group. However, CMR derived myocardial mass and functions do not correlate very well with BNP levels, patient status, physical exercise capacity or prognosis [87].

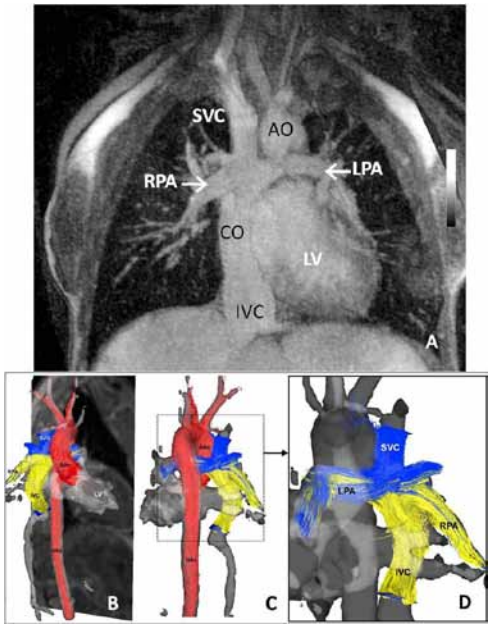

Figure 5: Fontan/ TCPC.
A: Reconstructed MR angiography of a patient with tricuspid atresia after completion of a total cavo pulmonary connection (TCPC). An extracardiac conduit (CO) connects the IVC to the right pulmonary artery (RPA), while the SVC is anastomosed directly to the RPA (Glenn anastomosis). B-D: 4D-Flow measurement of the Fontan tunnel and Glenn anstomosis (anterior (B), lateral (C) and posterior (D) views). Blood flow dynamics are visualized by vectors and blood from the IVC flows preferentially into the RPA (yellow), while the SVC drains into the LPA (blue). AO= aorta; LPA= left pulmonary artery, SVC/ IVC= superior/ inferior caval vein.
(B to D: courtesy of Prof. Michael Markl, Director Cardiovascular MR Research, Northwestern University, Chicago, IL, USA).

Miscellaneous lesions

Anomalous pulmonary venous return: Total and partial anomalous pulmonary venous return (APVR) can be diagnosed by CMR. Anatomic details and vessel aberrancy can be shown by MR angiography and dedicated 3D multiplanar reconstructions (Figure 6). The magnitude of the shunt volume can be assessed by velocity encoded flow measurements to quantify pulmonary and systemic blood flow (Qp and Qs) [88-90].

Recently, attempts have been undertaken to use 4D-velocity encoded cine MR imaging to improve diagnosis of APVR [91]. As with other 4D-flow studies, further data is needed to validate the use of this modality in the clinical setting.

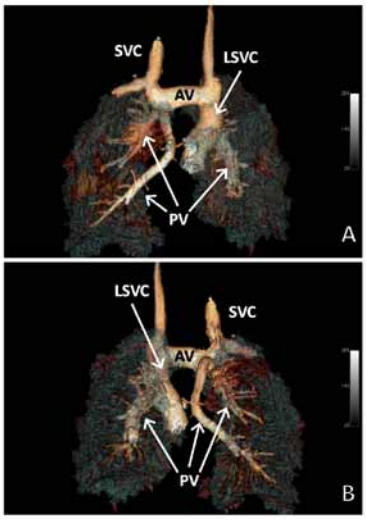

Figure 6: Total anomalous pulmonary venous return.
VR 3D reconstruction from MR angiography. Complex malformation with single ventricle and total anomalous pulmonary venous return. Drainage of the left pulmonary veins (PV) into the left SVC (LSVC) and the right PVs into the SVC. Both right and left SVC are connected by an enlarged anonymous vein (AV). A: anterior view, B: posterior view.

Ebstein's anomaly: Ebstein's Anomaly is a combination of an atrialized portion of the RV, tricuspid valve dysplasia with displacement of the septal origin of the valve towards the apex of more than 25mm and RV dysfunction (Figure 7). Few studies have addressed Ebstein's Anomaly by CMR and patient numbers are small. CMR is reliably used for verifying the initial diagnosis as well as follow up of RV function [92]. In a recent study, CMR derived ventricular and atrial measures were related to exercise capacity data. Ebstein patients exhibit increased RV sizes, atrialized portions of 25+/-24 ml/m^2 and decreased peak oxygen uptake (VO_2) of 65+/-20% of normal values. The atrialized RV volume from CMR was related to aerobic capacity and the volume of the atrialized RV can be used as a measure for the severity of the disease [93]. Attempts have been undertaken to classify severity of Ebstein's Anomaly prenatally by combination of fetal echocardiography and fetal MRI [94], but further steps are needed to implement this in clinical routine.

Cardiomyopathy: CMR is increasingly used to identify and asses risks in patients threatened by sudden cardiac death due to cardiomyopathies such as hypertrophic obstructive cardiomyopathy (HOCM) or arrhythmogenic rightventricular cardiomyoapthy (ARVC).

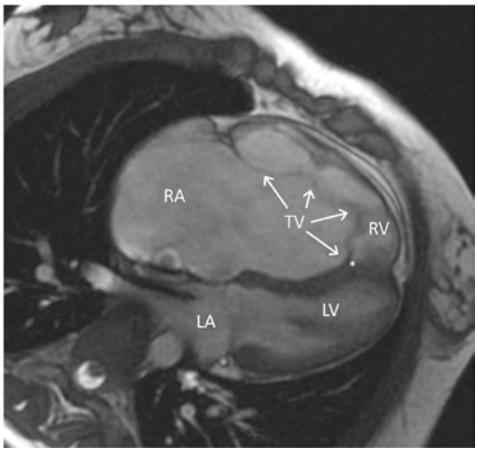

Figure 7: Ebstein's Anomaly.
SSFP-Image of an atrialised RV in Ebstein's anomaly. The very large right atrium (RA) is connected to the RV by a dysplastic tricuspid valve (TV) that is displaced towards the apex of the heart (*).

Arrhythmogenic right ventricular cardiomyopathy (ARVC): Arrhythmogenic right ventricular cardiomyopathy (ARVC) is a rare, but important cause for ventricular tachychardia and sudden cardiac death in children and young adults [95,96]. ARVC has been identified as agenetically determined disorder resulting in a progressing fibrofatty replacement of right ventricular cardiomyocytes [97]. The morphological correlate of ARVC is the development of wall aneurysms and segmental dilatation of the RV. The three typical sites of dysplasia are the RV apex, the inflow portion and the outflow tract ("triangle of dysplasia") whereas left ventricular involvement is possible but rare [98]. Due to the progressing nature of the disease, severity and clinical presentation may vary from unspecific symptoms like dizziness, palpitation and premature ventricular contractions (PVCs) to more severe findings like syncope, right ventricular heart failure, cardiomegaly and ventricular tachycardia [99]. It is not uncommon that in a previously healthy young adult the first and only documented symptom of ARVC is sudden cardiac death due to ventricular fibrillation [100].

CMR is an important diagnostic tool in the diagnosis of ARVC. It can reliably and noninvasively visualize abnormalities of the ventricular morphology including increased trabecularization, dilatation or aneurysm formation [101,102]. Using SSFP cine-sequences with high spatial and temporal resolution ventricular function and regional abnormalities in ventricular wall motion, such as akinesia, dyskinesia or dyssynchronous contraction can be assessed reliably [103,104].

The aforementioned pathological correlates of ARVC in CMR imaging are essential parts of the Revised Task Force Criteria for the diagnosis of ARVC that should be analyzed in any patient being suspected of ARVC [105]. Major CMR imaging criteria are regional right ventricular akinesia, dyskinesia or aneurysm formation in combination with either a pathological ratio of RV EDV to BSA (> 110 ml/m^2 in males and >100 ml/m^2 in females) or a reduced RV EF <40% [106,107]. Additionally myocardial LGE can be utilized for tissue characterization. However late enhancement analysis of the right ventricle can be more difficult than in the left ventricle due to its thinner walls and possible signal confusion with fat [108].

Hypertrophic cardiomyopathy (HCM)/ Hypertrophyic obstructive cardiomyopathy (HOCM): For the latest progress in MR

and HCM/ HOCM, we would like to refer the interested reader to recent and comprehensive review articles.

Summary

CMR is a very useful tool in the diagnosis, evaluation and management of patients with congenital heart disease (CHD). For CHD patients, the whole spectrum of CMR techniques is employed and delivers valuable information concerning ventricular and valve function, anatomy of malformed, surgically or interventionally corrected or palliated hearts and great vessel defects. It helps to correlate exercise capacity and prognostic factors such as scar formation, fibrosis or ventricle size. Depending on the individual defect, CMR complements other imaging modalities such as echocardiography and heart catheterization.

New MR techniques are being developed that in future might help to increase the role of CMR in the clinician's decision making. Among these are real time MRI, 3-/4D-Flow measurements, virtual surgery based on CMR data and the MRI heart catheterization laboratory. MRI based catheter interventions and measurements are possible in experimental settings. A future aim is the use of the advantages of CMR (high resolution, 3 dimensionality, non-x-ray) and combine them with those of the catheterization laboratory (measurement of pressures, oxygen saturation, interventions).

Overall, CMR already does play an ever increasing role in the management of CHD patients.

References

1. Gaca AM, Jaggers JJ, Dudley LT, Bisset GS 3rd (2008) Repair of congenital heart disease: a primer-part 1. Radiology 247: 617-631.
2. Gaca AM, Jaggers JJ, Dudley LT, Bisset GS 3rd (2008) Repair of congenital heart disease: a primer--Part 2. Radiology 248: 44-60.
3. Lai WW, Geva T, Shirali GS, Frommelt PC, Humes RA, et al. (2006) Guidelines and standards for performance of a pediatric echocardiogram: a report from the Task Force of the Pediatric Council of the American Society of Echocardiography. J Am Soc Echocardiogr 19: 1413-1430.
4. Lopez L, Colan SD, Frommelt PC, Ensing GJ, Kendall K, et al. (2010) Recommendations for quantification methods during the performance of a pediatric echocardiogram: a report from the Pediatric Measurements Writing Group of the American Society of Echocardiography Pediatric and Congenital Heart Disease Council. J Am Soc Echocardiogr 23: 465-495, quiz 576-577.
5. Ntsinjana HN, Hughes ML, Taylor AM (2011) The Role of Cardiovascular Magnetic Resonance in Pediatric Congenital Heart Disease. J Cardiovasc Magn Reson 13: 51.
6. Powell AJ, Geva T (2000) Blood flow measurement by magnetic resonance imaging in congenital heart disease. Pediatr Cardiol 21: 47-58.
7. van den Bosch AE, Robbers-Visser D, Krenning BJ, Voormolen MM, McGhie JS, et al. (2006) Real-time transthoracic three-dimensional echocardiographic assessment of left ventricular volume and ejection fraction in congenital heart disease. J Am Soc Echocardiogr 19: 1-6.
8. Riesenkampff E, Rietdorf U, Wolf I, Schnackenburg B, Ewert P, et al. (2009) The practical clinical value of three-dimensional models of complex congenitally malformed hearts. J Thorac Cardiovasc Surg 138: 571-580.
9. Kilner PJ (2011) The role of cardiovascular magnetic resonance in adults with congenital heart disease. Prog Cardiovasc Dis 54: 295-304.
10. Debl K, Djavidani B, Buchner S, Heinicke N, Poschenrieder F, et al. (2009) Quantification of left-to-right shunting in adult congenital heart disease: phase-contrast cine MRI compared with invasive oximetry. Br J Radiol 82: 386-391.
11. Floemer F, Ulmer HE, Brockmeier K (2000) Images in congenital heart disease. Use of 3D volume rendered magnetic resonance angiography to demonstrate a cervical aortic arch. Cardiol Young 10: 423-424.
12. Hunold P, Schlosser T, Vogt FM, Eggebrecht H, Schmermund A, et al. (2005) Myocardial late enhancement in contrast-enhanced cardiac MRI: distinction between infarction scar and non-infarction-related disease. AJR Am J Roentgenol 184: 1420-1426.
13. Babu-Narayan SV, Kilner PJ, Li W, Moon JC, Goktekin O, et al. (2006) Ventricular fibrosis suggested by cardiovascular magnetic resonance in adults with repaired tetralogy of fallot and its relationship to adverse markers of clinical outcome. Circulation 113: 405-413.
14. Babu-Narayan SV, Goktekin O, Moon JC, Broberg CS, Pantely GA, et al. (2005) Late gadolinium enhancement cardiovascular magnetic resonance of the systemic right ventricle in adults with previous atrial redirection surgery for transposition of the great arteries. Circulation 111: 2091-2098.
15. Rathod RH, Prakash A, Powell AJ, Geva T (2010) Myocardial fibrosis identified by cardiac magnetic resonance late gadolinium enhancement is associated with adverse ventricular mechanics and ventricular tachycardia late after Fontan operation. J Am Coll Cardiol 55: 1721-1728.
16. O'Hanlon R, Grasso A, Roughton M, Moon JC, Clark S, et al. (2010) Prognostic significance of myocardial fibrosis in hypertrophic cardiomyopathy. J Am Coll Cardiol 56: 867-874.
17. Zemrak F, Petersen SE (2011) Late Gadolinium Enhancement CMR Predicts Adverse Cardiovascular Outcomes and Mortality in Patients With Coronary Artery Disease: Systematic Review and Meta-Analysis. Prog Cardiovasc Dis 54: 215-229.
18. Manso B, Castellote A, Dos L, Casaldaliga J (2010) Myocardial perfusion magnetic resonance imaging for detecting coronary function anomalies in asymptomatic paediatric patients with a previous arterial switch operation for the transposition of great arteries. Cardiol Young 20: 410-417.
19. Brix L, Ringgaard S, Rasmusson A, Sorensen TS, Kim WY (2009) Three dimensional three component whole heart cardiovascular magnetic resonance velocity mapping: comparison of flow measurements from 3D and 2D acquisitions. J Cardiovasc Magn Reson 11: 3.
20. Markl M, Geiger J, Stiller B, Arnold R (2011) Impaired continuity of flow in congenital heart disease with single ventricle physiology. Interact Cardiovasc Thorac Surg 12: 87-90.
21. Nordmeyer S, Riesenkampff E, Crelier G, Khasheei A, Schnackenburg B, et al. (2010) Flow-sensitive four-dimensional cine magnetic resonance imaging for offline blood flow quantification in multiple vessels: a validation study. J Magn Reson Imaging 32: 677-683.
22. Pedra CA, Fleishman C, Pedra SF, Cheatham JP (2011) New imaging modalities in the catheterization laboratory. Curr Opin Cardiol 26: 86-93.
23. Neizel M, Kramer N, Schutte A, Schnackenburg B, Kruger S, et al. (2010) Magnetic resonance imaging of the cardiac venous system and magnetic resonance-guided intubation of the coronary sinus in swine: a feasibility study. Invest Radiol 45: 502-506.
24. Neizel M, Kramer N, Bonner F, Schutte A, Kruger S, et al. (2010) Rapid right ventricular pacing with MR-compatible pacemaker lead for MR-guided aortic balloon valvuloplasty in swine. Radiology 255: 799-804.
25. Ratnayaka K, Raman VK, Faranesh AZ, Sonmez M, Kim JH, et al. (2009) Antegrade percutaneous closure of membranous ventricular septal defect using X-ray fused with magnetic resonance imaging. JACC Cardiovasc Interv 2: 224-230.
26. Kos S, Huegli R, Hofmann E, Quick HH, Kuehl H, et al. (2009) First magnetic resonance imaging-guided aortic stenting and cava filter placement using a polyetheretherketone-based magnetic resonance imaging-compatible guidewire in swine: proof of concept. Cardiovasc Intervent Radiol 32: 514-521.
27. Kos S, Huegli R, Hofmann E, Quick HH, Kuehl H, et al. (2009) Feasibility of real-time magnetic resonance-guided angioplasty and stenting of renal arteries in vitro and in Swine, using a new polyetheretherketone-based magnetic resonance-compatible guidewire. Invest Radiol 44: 234-241.
28. Kos S, Huegli R, Hofmann E, Quick HH, Kuehl H, et al. (2009) MR-compatible polyetheretherketone-based guide wire assisting MR-guided stenting of iliac and supraaortic arteries in swine: feasibility study. Minim Invasive Ther Allied Technol 18: 181-188.
29. Raval AN, Telep JD, Guttman MA, Ozturk C, Jones M, et al. (2005) Real-time magnetic resonance imaging-guided stenting of aortic coarctation with commercially available catheter devices in Swine. Circulation 112: 699-706.
30. Schmitt B, Steendijk P, Lunze K, Ovroutski S, Falkenberg J, et al. (2009) Integrated assessment of diastolic and systolic ventricular function using

diagnostic cardiac magnetic resonance catheterization: validation in pigs and application in a clinical pilot study. JACC Cardiovasc Imaging 2: 1271-1281.

31. George AK, Faranesh AZ, Ratnayaka K, Derbyshire JA, Lederman RJ, et al. (2011) Virtual dye angiography: Flow visualization for MRI-guided interventions. Magn Reson Med.
32. Saikus CE, Ratnayaka K, Barbash IM, Colyer JH, Kocaturk O, et al. (2011) MRI-guided vascular access with an active visualization needle. J Magn Reson Imaging 34: 1159-1166.
33. Wu V, Barbash IM, Ratnayaka K, Saikus CE, Sonmez M, et al. (2011) Adaptive noise cancellation to suppress electrocardiography artifacts during real-time interventional MRI. J Magn Reson Imaging 33: 1184-1193.
34. Ratnayaka K, Faranesh AZ, Guttman MA, Kocaturk O, Saikus CE, et al. (2008) Interventional cardiovascular magnetic resonance: still tantalizing. J Cardiovasc Magn Reson 10: 62.
35. Moore P (2005) MRI-guided congenital cardiac catheterization and intervention: the future? Catheter Cardiovasc Interv 66: 1-8.
36. Greil GF, Wolf I, Kuettner A, Fenchel M, Miller S, et al. (2007) Stereolithographic reproduction of complex cardiac morphology based on high spatial resolution imaging. Clin Res Cardiol 96: 176-185.
37. Sorensen TS, Beerbaum P, Mosegaard J, Rasmusson A, Schaeffter T, et al. (2008) Virtual cardiotomy based on 3-D MRI for preoperative planning in congenital heart disease. Pediatr Radiol 38: 1314-1322.
38. Sorensen TS, Beerbaum P, Mosegaard J, Greil GF (2009) Developing and evaluating virtual cardiotomy for preoperative planning in congenital heart disease. Stud Health Technol Inform 142: 340-345.
39. Oosterhof T, van Straten A, Vliegen HW, Meijboom FJ, van Dijk AP, et al. (2007) Preoperative thresholds for pulmonary valve replacement in patients with corrected tetralogy of Fallot using cardiovascular magnetic resonance. Circulation 116: 545-551.
40. Sarikouch S, Peters B, Gutberlet M, Leismann B, Kelter-Kloepping A, et al. (2010) Sex-specific pediatric percentiles for ventricular size and mass as reference values for cardiac MRI: assessment by steady-state free-precession and phase-contrast MRI flow. Circ Cardiovasc Imaging 3: 65-76.
41. Sarikouch S, Koerperich H, Dubowy KO, Boethig D, Boettler P, et al. (2011) Impact of Gender and Age on Cardiovascular Function Late After Repair of Tetralogy of Fallot: Percentiles Based on Cardiac Magnetic Resonance. Circ Cardiovasc Imaging 4: 703-711.
42. Spiewak M, Biernacka EK, Malek LA, Petryka J, Kowalski M, et al. (2011) Right ventricular outflow tract obstruction as a confounding factor in the assessment of the impact of pulmonary regurgitation on the right ventricular size and function in patients after repair of tetralogy of Fallot. J Magn Reson Imaging 33: 1040-1046.
43. Park SJ, On YK, Kim JS, Park SW, Yang JH, et al. (2011) Relation of Fragmented QRS Complex to Right Ventricular Fibrosis Detected by Late Gadolinium Enhancement Cardiac Magnetic Resonance in Adults With Repaired Tetralogy of Fallot. Am J Cardiol 109: 110-115.
44. Kempny A, Diller GP, Orwat S, Kaleschke G, Kerckhoff G, et al. (2010) Right ventricular-left ventricular interaction in adults with Tetralogy of Fallot: A combined cardiac magnetic resonance and echocardiographic speckle tracking study. Int J Cardiol 154: 259-264.
45. Riesenkampff E, Mengelkamp L, Mueller M, Kropf S, Abdul-Khaliq H, et al. (2010) Integrated analysis of atrioventricular interactions in tetralogy of Fallot. Am J Physiol Heart Circ Physiol 299: H364-371.
46. Morcos P, Vick GW 3rd, Sahn DJ, Jerosch-Herold M, Shurman A (2009) Correlation of right ventricular ejection fraction and tricuspid annular plane systolic excursion in tetralogy of Fallot by magnetic resonance imaging. Int J Cardiovasc Imaging 25: 263-270.
47. Bodhey NK, Beerbaum P, Sarikouch S, Kropf S, Lange P, et al. (2008) Functional analysis of the components of the right ventricle in the setting of tetralogy of Fallot. Circ Cardiovasc Imaging 1: 141-147.
48. Iriart X, Montaudon M, Lafitte S, Chabaneix J, Reant P, et al. (2009) Right ventricle three-dimensional echography in corrected tetralogy of fallot: accuracy and variability. Eur J Echocardiogr 10: 784-792.
49. Romeih S, Kroft LJ, Bokenkamp R, Schalij MJ, Grotenhuis H, et al. (2009) Delayed improvement of right ventricular diastolic function and regression of right ventricular mass after percutaneous pulmonary valve implantation in patients with congenital heart disease. Am Heart J 158: 40-46.
50. Jenkins NP, Ward C (1999) Coarctation of the aorta: natural history and outcome after surgical treatment. Qjm 92: 365-371.
51. Aboulhosn J, Levi DS, Child JS (2011) Common congenital heart disorders in adults: percutaneous therapeutic procedures. Curr probl Cardiol 36: 263-284.
52. Fruh S, Knirsch W, Dodge-Khatami A, Dave H, Pretre R, et al. (2011) Comparison of surgical and interventional therapy of native and recurrent aortic coarctation regarding different age groups during childhood. Eur J Cardiothorac Surg 39: 898-904.
53. Mohan UR, Danon S, Levi D, Connolly D, Moore JW (2009) Stent implantation for coarctation of the aorta in children <30 kg. JACC Cardiovascular interventions 2: 877-883.
54. Tsai SF, Trivedi M, Boettner B, Daniels CJ (2011) Usefulness of screening cardiovascular magnetic resonance imaging to detect aortic abnormalities after repair of coarctation of the aorta. Am J Cardiol 107: 297-301.
55. Puranik R, Tsang VT, Puranik S, Jones R, Cullen S, et al. (2009) Late magnetic resonance surveillance of repaired coarctation of the aorta. Eur J Cardiothorac Surg 36: 91-95; discussion 95.
56. Mendelsohn AM, Crowley DC, Lindauer A, Beekman RH 3rd (1992) Rapid progression of aortic aneurysms after patch aortoplasty repair of coarctation of the aorta. J Am Coll Cardiol 20: 381-385.
57. Piciucchi S, Goodman LR, Earing M, Nicolosi A, Almassi H, et al. (2008) Aortic aneurysms: delayed complications of coarctation of the aorta repair using Dacron patch aortoplasty. J Thorac Imaging 23: 278-283.
58. Cantinotti M, Hegde S, Bell A, Razavi R (2008) Diagnostic role of magnetic resonance imaging in identifying aortic arch anomalies. Congenit Heart Dis 3: 117-123.
59. Hom JJ, Ordovas K, Reddy GP (2008) Velocity-encoded cine MR imaging in aortic coarctation: functional assessment of hemodynamic events. Radiographics 28: 407-416.
60. Secchi F, Iozzelli A, Papini GD, Aliprandi A, Di Leo G, et al. (2009) MR imaging of aortic coarctation. Radiol Med 114: 524-537.
61. Teo LL, Cannell T, Babu-Narayan SV, Hughes M, Mohiaddin RH (2011) Prevalence of associated cardiovascular abnormalities in 500 patients with aortic coarctation referred for cardiovascular magnetic resonance imaging to a tertiary center. Pediatr Cardiol 32: 1120-1127.
62. Ou P, Mousseaux E, Celermajer DS, Pedroni E, Vouhe P, et al. (2006) Aortic arch shape deformation after coarctation surgery: effect on blood pressure response. J Thorac Cardiovasc Surg 132: 1105-1111.
63. Ou P, Celermajer DS, Mousseaux E, Giron A, Aggoun Y, et al. (2007) Vascular remodeling after "successful" repair of coarctation: impact of aortic arch geometry. J Am Coll Cardiol 49: 883-890.
64. Lashley D, Curtin J, Malcolm P, Clark A, Freeman L (2007) Aortic arch morphology and late systemic hypertension following correction of coarctation of aorta. Congenit Heart Dis 2: 410-415.
65. Muzzarelli S, Meadows AK, Ordovas KG, Hope MD, Higgins CB, et al. (2011) Prediction of Hemodynamic Severity of Coarctation by Magnetic Resonance Imaging. Am J Cardiol 108: 1335-1340.
66. Hope MD, Meadows AK, Hope TA, Ordovas KG, Saloner D, et al. (2010) Clinical evaluation of aortic coarctation with 4D flow MR imaging. J Magn Reson Imaging 31: 711-718.
67. Hope MD, Meadows AK, Hope TA, Ordovas KG, Reddy GP, et al. (2008) Images in cardiovascular medicine. Evaluation of bicuspid aortic valve and aortic coarctation with 4D flow magnetic resonance imaging. Circulation 117: 2818-2819.
68. Bock J, Frydrychowicz A, Lorenz R, Hirtler D, Barker AJ, et al. (2011) In vivo noninvasive 4D pressure difference mapping in the human aorta: phantom comparison and application in healthy volunteers and patients. Magn Reson Med 66: 1079-1088.
69. Nordmeyer J, Gaudin R, Tann OR, Lurz PC, Bonhoeffer P, et al. (2010) MRI may be sufficient for noninvasive assessment of great vessel stents: an in vitro comparison of MRI, CT, and conventional angiography. AJR Am J Roentgenol 195: 865-871.
70. Rasche V, Oberhuber A, Trumpp S, Bornstedt A, Orend KH, et al. (2011) MRI assessment of thoracic stent grafts after emergency implantation in multi trauma patients: a feasibility study. Eur Radiol 21: 1397-1405.

71. Sridharan S, Yates R, Taylor AM (2005) Optimizing imaging after coarctation stenting: the clinical utility of multidetector computer tomography. Catheter Cardiovasc Interv 66: 420-423.

72. Thanopoulos BV, Douskou M, Giannakoulas G (2010) Multislice computed tomography after stent implantation for aortic coarctation. Eur Heart J 31: 2270.

73. Iezzi R, Dattesi R, Pirro F, Nestola M, Santoro M, et al. (2011) CT angiography in stent-graft sizing: impact of using inner vs. outer wall measurements of aortic neck diameters. J Endovasc Ther 18: 280-288.

74. Coogan JS, Chan FP, Taylor CA, Feinstein JA (2011) Computational fluid dynamic simulations of aortic coarctation comparing the effects of surgical- and stent-based treatments on aortic compliance and ventricular workload. Catheter Cardiovasc Interv 77: 680-691.

75. Ho JG, Cohen MD, Ebenroth ES, Schamberger MS, Cordes TM, et al. (2011) Comparison between Transthoracic Echocardiography and Cardiac Magnetic Resonance Imaging in Patients Status Post Atrial Switch Procedure. Congenit Heart Dis.

76. Giardini A, Khambadkone S, Taylor A, Derrick G (2010) Effect of abnormal pulmonary flow distribution on ventilatory efficiency and exercise capacity after arterial switch operation for transposition of great arteries. Am J Cardiol 106: 1023-1028.

77. Plymen CM, Hughes ML, Picaut N, Panoulas VF, Macdonald ST, et al. (2010) The relationship of systemic right ventricular function to ECG parameters and NT-proBNP levels in adults with transposition of the great arteries late after Senning or Mustard surgery. Heart 96: 1569-1573.

78. Fratz S, Hager A, Busch R, Kaemmerer H, Schwaiger M, et al. (2008) Patients after atrial switch operation for transposition of the great arteries can not increase stroke volume under dobutamine stress as opposed to patients with congenitally corrected transposition. Circ J 72: 1130-1135.

79. Tulevski, II, van der Wall EE, Groenink M, Dodge-Khatami A, Hirsch A, et al. (2002) Usefulness of magnetic resonance imaging dobutamine stress in asymptomatic and minimally symptomatic patients with decreased cardiac reserve from congenital heart disease (complete and corrected transposition of the great arteries and subpulmonic obstruction). Am J Cardiol 89: 1077-1081.

80. Giardini A, Lovato L, Donti A, Formigari R, Oppido G, et al. (2006) Relation between right ventricular structural alterations and markers of adverse clinical outcome in adults with systemic right ventricle and either congenital complete (after Senning operation) or congenitally corrected transposition of the great arteries. Am J Cardiol 98: 1277-1282.

81. Pettersen E, Lindberg H, Smith HJ, Smevik B, Edvardsen T, et al. (2008) Left ventricular function in patients with transposition of the great arteries operated with atrial switch. Pediatr Cardiol 29: 597-603.

82. Ladouceur M, Kachenoura N, Lefort M, Redheuil A, Bonnet D, et al. (2011) Structure and function of the ascending aorta in palliated transposition of the great arteries. Int J Cardiol.

83. Ovroutski S, Nordmeyer S, Miera O, Ewert P, Klimes K, et al. (2011) Caval flow reflects Fontan hemodynamics: quantification by magnetic resonance imaging. Clin Res Cardiol.

84. Klimes K, Abdul-Khaliq H, Ovroutski S, Hui W, Alexi-Meskishvili V, et al. (2007) Pulmonary and caval blood flow patterns in patients with intracardiac and extracardiac Fontan: a magnetic resonance study. Clin Res Cardiol 96: 160-167.

85. Schmitt B, Steendijk P, Ovroutski S, Lunze K, Rahmanzadeh P, et al. (2010) Pulmonary vascular resistance, collateral flow, and ventricular function in patients with a Fontan circulation at rest and during dobutamine stress. Circ Cardiovasc Imaging 3: 623-631.

86. Sundareswaran KS, Haggerty CM, de Zelicourt D, Dasi LP, Pekkan K, et al. (2011) Visualization of flow structures in Fontan patients using 3-dimensional phase contrast magnetic resonance imaging. J Thorac Cardiovasc Surg.

87. Atz AM, Zak V, Breitbart RE, Colan SD, Pasquali SK, et al. (2011) Factors associated with serum brain natriuretic peptide levels after the Fontan procedure. Congenit Heart Dis 6: 313-321.

88. Riesenkampff EM, Schmitt B, Schnackenburg B, Huebler M, Alexi-Meskishvili V, et al. (2009) Partial anomalous pulmonary venous drainage in young pediatric patients: the role of magnetic resonance imaging. Pediatr Cardiol 30: 458-464.

89. Dellegrottaglie S, Pedrotti P, Pedretti S, Mauri F, Roghi A (2008) Atrial septal defect combined with partial anomalous pulmonary venous return: complete anatomic and functional characterization by cardiac magnetic resonance. J Cardiovasc Med (Hagerstown) 9: 1184-1186.

90. Beerbaum P, Parish V, Bell A, Gieseke J, Korperich H, et al. (2008) Atypical atrial septal defects in children: noninvasive evaluation by cardiac MRI. Pediatr Radiol 38: 1188-1194.

91. Nordmeyer S, Berger F, Kuehne T, Riesenkampff E (2011) Flow-sensitive four-dimensional magnetic resonance imaging facilitates and improves the accurate diagnosis of partial anomalous pulmonary venous drainage. Cardiol Young 21: 528-535.

92. Yalonetsky S, Tobler D, Greutmann M, Crean AM, Wintersperger BJ, et al. (2011) Cardiac magnetic resonance imaging and the assessment of ebstein anomaly in adults. Am J Cardiol 107: 767-773.

93. Tobler D, Yalonetsky S, Crean AM, Granton JT, Burchill L, et al. (2011) Right heart characteristics and exercise parameters in adults with Ebstein anomaly: New perspectives from cardiac magnetic resonance imaging studies. Int J Cardiol.

94. Nathan AT, Marino BS, Dominguez T, Tabbutt S, Nicolson S, et al. (2010) Tricuspid valve dysplasia with severe tricuspid regurgitation: fetal pulmonary artery size predicts lung viability in the presence of small lung volumes. Fetal Diagn Ther 27: 101-105.

95. Hamilton RM (2009) Arrhythmogenic right ventricular cardiomyopathy. Pacing Clin Electrophysiol 32 Suppl 2: S44-51.

96. Sen-Chowdhry S, Morgan RD, Chambers JC, McKenna WJ (2010) Arrhythmogenic cardiomyopathy: etiology, diagnosis, and treatment. Annu Rev Med 61: 233-253.

97. Azaouagh A, Churzidse S, Konorza T, Erbel R (2011) Arrhythmogenic right ventricular cardiomyopathy/dysplasia: a review and update. Clin Res Cardiol 100: 383-394.

98. Marcus FI, Fontaine GH, Guiraudon G, Frank R, Laurenceau JL, et al. (1982) Right ventricular dysplasia: a report of 24 adult cases. Circulation 65: 384-398.

99. McRae AT 3rd, Chung MK, Asher CR (2001) Arrhythmogenic right ventricular cardiomyopathy: a cause of sudden death in young people. Cleveland Clinic journal of medicine 68: 459-467.

100. Corrado D, Basso C, Thiene G, McKenna WJ, Davies MJ, et al. (1997) Spectrum of clinicopathologic manifestations of arrhythmogenic right ventricular cardiomyopathy/dysplasia: a multicenter study. J Am Coll Cardiol 30: 1512-1520.

101. Bluemke DA, Krupinski EA, Ovitt T, Gear K, Unger E, et al. (2003) MR Imaging of arrhythmogenic right ventricular cardiomyopathy: morphologic findings and interobserver reliability. Cardiology 99: 153-162.

102. Tandri H, Daya SK, Nasir K, Bomma C, Lima JA, et al. (2006) Normal reference values for the adult right ventricle by magnetic resonance imaging. Am J Cardiol 98: 1660-1664.

103. Maksimovic R, Ekinci O, Reiner C, Bachmann GF, Seferovic PM, et al. (2006) The value of magnetic resonance imaging for the diagnosis of arrhythmogenic right ventricular cardiomyopathy. European radiology 16: 560-568.

104. Tandri H, Macedo R, Calkins H, Marcus F, Cannom D, et al. (2008) Role of magnetic resonance imaging in arrhythmogenic right ventricular dysplasia: insights from the North American arrhythmogenic right ventricular dysplasia (ARVD/C) study. Am Heart J 155: 147-153.

105. Sen-Chowdhry S, Prasad SK, Syrris P, Wage R, Ward D, et al. (2006) Cardiovascular magnetic resonance in arrhythmogenic right ventricular cardiomyopathy revisited: comparison with task force criteria and genotype. J Am Coll Cardiol 48: 2132-2140.

106. Marcus FI, McKenna WJ, Sherrill D, Basso C, Bauce B, et al. (2010) Diagnosis of arrhythmogenic right ventricular cardiomyopathy/dysplasia: proposed modification of the task force criteria. Circulation 121: 1533-1541.

107. McKenna WJ, Thiene G, Nava A, Fontaliran F, Blomstrom-Lundqvist C, et al. (1994) Diagnosis of arrhythmogenic right ventricular dysplasia/ cardiomyopathy. Task Force of the Working Group Myocardial and Pericardial Disease of the European Society of Cardiology and of the Scientific Council on Cardiomyopathies of the International Society and Federation of Cardiology. Br Heart J 71: 215-218.

108. Tandri H, Saranathan M, Rodriguez ER, Martinez C, Bomma C, et al. (2005) Noninvasive detection of myocardial fibrosis in arrhythmogenic right ventricular cardiomyopathy using delayed-enhancement magnetic resonance imaging. J Am Coll Cardiol 45: 98-103.